



1 **Atmospheric deposition of organic matter at a remote site in the**
2 **Central Mediterranean Sea: implications for marine ecosystem**

3 Yuri Galletti¹, Silvia Becagli², Alcide di Sarra³, Margherita Gonnelli¹, Elvira Pulido-Villena⁴,
4 Damiano M. Sferlazzo³, Rita Traversi², Stefano Vestri¹, Chiara Santinelli¹

5 ¹CNR, Biophysics Institute, Pisa, Italy

6 ²Department of Chemistry "Ugo Schiff", University of Florence, Italy

7 ³Laboratory for Observations and Analyses of the Earth and Climate (SSPT-PROTER-OAC), ENEA, Rome, Italy

8 ⁴Institut Méditerranéen d'Océanologie, MIO - Marseille, France

9

10 Correspondence to: Yuri Galletti (yuri.galletti@pi.ibf.cnr.it)

11

12 **Abstract.** Atmospheric fluxes of dissolved organic matter (DOM) were studied for the first time at the Island of
13 Lampedusa, a remote site in the Central Mediterranean Sea (Med Sea), close to the Sahara desert, between March 19th
14 2015 and April 1st 2017. The main goals of this work are: to quantify total atmospheric deposition of DOM in this area
15 and to evaluate the impact of dust deposition on DOM dynamics in the surface waters of the Mediterranean Sea. Our
16 data show high variability in DOM deposition rates without a clear seasonality and allow to estimate a dissolved
17 organic carbon (DOC) input from the atmosphere of 120.7 mmol DOC m⁻² y⁻¹. Over the entire time-series, the average
18 dissolved organic phosphorous (DOP) and dissolved organic nitrogen (DON) contributions to the total dissolved pools
19 were 40% and 26%, respectively. The data on atmospheric elemental ratios also show that each deposition event is
20 characterized by a specific elemental ratio, suggesting a high variability in DOM composition and the presence of
21 multiple sources. This study indicates that the organic substances transported by Saharan dust at Lampedusa site mainly
22 have natural origin, especially from sea spray and that Saharan dust can be an important carrier of organic substances,
23 even if the load of DOC associated with dust is highly variable. Our estimates suggest that atmospheric input has an
24 impact to the Med Sea larger than to the global ocean and that DOC fluxes from the atmosphere to the Med Sea can be
25 up to 6-fold larger than river input. Longer time series, combined with a modelling effort, are therefore mandatory in
26 order to investigate the response of DOM dynamics in the Med Sea to the change in aerosol deposition pattern due to
27 the effect of climate change.

28

29 **1. Introduction**

30 The Mediterranean Sea (Med Sea) is the largest semi-enclosed basin and one of the most oligotrophic areas in the
31 world. It is very sensitive to natural variations in the atmosphere-ocean interactions (Mermex group, 2011). Organic
32 matter and nutrients of natural and anthropic origin, are continuously exchanged between the ocean and the atmosphere,
33 affecting biogeochemical cycles and the marine ecosystem. The Med Sea receives anthropogenic aerosols from the
34 northern regions, which are characterized by the presence of important industrial sites, representing relevant sources of
35 organic substances to the atmosphere (Guerzoni and Chester, 1996). In addition, the Sahara desert is an intermittent
36 source of mineral dust, that can transport nutrients and organic carbon to the Basin (Goudie and Middleton, 2001;
37 Prospero et al., 2005; Vincent et al., 2016). Atmospheric deposition of nutrients (N and P) strongly influences the
38 marine biogeochemical cycles of the Med Sea, it has therefore received attention in the last 30 years (Migon et al.,
39 1989; Herut et al., 2002; Ridame and Guieu, 2002; Markaki et al., 2003, 2010; Pulido-Villena et al., 2008; Djaoudi et
40 al., 2018). Compared to inorganic nutrients, there is still very few data on the atmospheric deposition of Dissolved
41 Organic Carbon (DOC) to the surface ocean, both at the global and local scale. Organic carbon can be removed from



42 the atmosphere via both wet and dry deposition (Iavorivska et al., 2016). At the global scale, wet deposition transfers
43 about 306-580 Tg DOC yr⁻¹ to the surface of the Earth (Willey et al., 2000; Kanakidou et al., 2012). These values
44 correspond to almost half of the DOC delivered to the oceans by rivers annually (IPCC, 2014). Atmospheric deposition
45 can therefore affect regional C cycling, radiative forcing, and human health (Yan and Kim, 2012; Decina et al., 2018).
46 In addition, the expected increase in ocean stratification due to the global warming will enhance the impact of
47 atmospheric inputs in the surface ecosystem (Kanakidou et al., 2012). The potential magnitude of atmospheric DOC
48 inputs to open waters and the importance of its role in the carbon cycle highlight the need for a better and robust
49 estimation of DOC deposition.

50 In the last years, a few studies have reported data on atmospheric deposition of DOC to the Med Sea. Total (dry + wet)
51 atmospheric deposition was studied in North-Western Med Sea in 2006 (Pulido-Villena et al., 2008) and in 2015
52 (Djaoudi et al., 2018) with contrasting results. In the first study, the highest DOC flux was observed in correspondence
53 with a Saharan dust storm, suggesting a combination of heterogeneous reactions between organic matter and mineral
54 dust in the troposphere. In the second study, the Saharan rain event coincided with a minimum in DOC input,
55 suggesting the presence of an aerosol poorly enriched in organic matter (Djaoudi et al., 2018). These studies were
56 conducted in coastal areas affected by human activities. Direct measurements of total OC (TOC) in rainwater were
57 performed at the Crete Island (Eastern Mediterranean; Economou and Mihalopoulos, 2002). This study did not take into
58 consideration dry deposition. None of the papers cited has studied atmospheric inputs in remote sites, far from possible
59 pollution sources and/or large cities.

60 The main goals of this study are: (1) to quantify total atmospheric deposition of DOC, DON and DOP at the island of
61 Lampedusa, representative of the remote marine environment of the central Med Sea; (2) to investigate the contribution
62 of natural and anthropogenic sources in atmospheric DOC; (3) to estimate the impact of atmospheric deposition on
63 marine ecosystem.

64

65 **2. Materials and methods**

66 **2.1 Sampling site**

67 Bulk atmospheric deposition (dry and wet) was collected at the Station for Climate Observations (35.52°N, 12.63°E),
68 maintained by ENEA (the Italian National Agency for New Technologies, Energy and Sustainable Economic
69 Development), on the island of Lampedusa, Italy (Fig. 1), (<http://www.lampedusa.enea.it/>).

70 An interesting aspect of the Med Sea is related to Dissolved Organic Matter (DOM) stoichiometry. Mediterranean DOC
71 and Dissolved Organic Nitrogen (DON) concentrations and their ratios are similar to those reported for the global ocean
72 (Pujo-Pay et al., 2011; Santinelli, 2015). In the surface waters (0-100 m), C:N:P ratios show that Mediterranean DOM is
73 depleted in Dissolved Organic phosphorous (DOP). The study of C:N:P ratio of DOM in atmospheric deposition is
74 important in order to estimate the relative contribution of atmospheric DOM input to the inventory of the surface DOM
75 pool and to understand the fate of the three elements in the water column.

76 This study reports the results of analyses on deposition collected at Lampedusa island (35.52°N, 12.63°E) located in
77 central Med Sea. Lampedusa is located in an ideal position for the study of atmospheric DOC fluxes to the open Med
78 Sea. The site is interesting, in particular, to investigate the mineral dust contribution (mean dust deposition=7.4 g
79 year⁻¹, Vincent et al., 2016) to DOC deposition. Lampedusa is a flat island far from large islands or continental areas and
80 from relevant pollutant sources. Although influences from ship traffic emissions (Becagli et al., 2012, 2017), volcanic



81 aerosols (Sellitto et al., 2017), forest fires (Pace et al., 2005), and regional pollution (Pace et al., 2006), have been
82 documented, their contribution to the total aerosol load is small, and Lampedusa may be taken as representative for the
83 remote marine environment of the central Med Sea. The importance of this study area is that previous work on DOC
84 atmospheric deposition to the Med was essentially confined to the coastal areas, less representative of what is actually
85 arriving to the open Med Sea. Measurements at Lampedusa provide additional important information on the deposition
86 in the open Med Sea.

87 In addition to deposition, also measurements of PM₁₀ amount and chemical composition, routinely performed at
88 Lampedusa, are used in this study.

89

90 **2.2. Atmospheric deposition sampler**

91 The sampler (Fig. 1) was positioned on the roof of the ENEA climatic station located on a 45 m a.s.l. plateau on the
92 north-eastern coast of Lampedusa. A total of 41 samples were collected between March 19th 2015 and April 1st 2017,
93 every 15 days or immediately after strong rain or dust storm events. Due to logistic constraints, 9 sampling periods were
94 longer than 20 days. The deposition sampler is similar to those successfully employed in previous studies (Pulido-
95 Villena et al., 2008; Markaki et al. 2010; De Vicente et al., 2012). It is composed by a 10 L Polycarbonate bottle, with a
96 polyethylene funnel attached on the top; a 20 µm mesh covers the funnel stem in order to prevent contamination by
97 insects or organic debris. In case of wet deposition, the amount of water in the sampler was weighted then it was
98 collected in 250 ml polycarbonate bottles and immediately frozen. In case of dry deposition, the sampler was rinsed
99 with 250 mL of ultrapure MilliQ water, the sample was then collected in 250 ml polycarbonate bottles and immediately
100 frozen. A detailed description of sampling periods, deposition types, and collected volumes is reported in Table 1.

101 Samples for DOC, DON and DOP were thawed and filtered through a sterile 0.2 µm Nylon filter pre-washed with 300
102 ml of ultrapure water to avoid any contamination. Filtered samples were frozen until the analysis. Before the analysis,
103 samples were brought to room temperature (24 °C).

104 The concentration of soluble ions metals was measured on the samples filtered on quartz filters. These filters have low
105 blanks level for metals and ions respect to the determined concentration both in the soluble and particulate fraction. Just
106 after filtration the sample was divided in two portions, one for ionic content and the other for metal content, the latter
107 was spiked by 0.1 mL of sub-boiled distilled (s.b.) HNO₃ to preserve the metals in their soluble form. Samples was keep
108 refrigerate at +4°C until the analysis.

109

110 **2.3 DOC analysis**

111 DOC analysis were carried by a Shimadzu TOC-VCSN, equipped with a quartz combustion column filled with 1.2% Pt
112 on alumina pillows of ~2 mm diameter. Samples were first acidified with 2N HCl and bubbled for 3 min with CO₂-free
113 ultra-high purity air in order to remove the inorganic carbon. Replicate injections were performed until the analytical
114 precision was lower than 1%. A five-point linear calibration curve was determined with standard solutions of potassium
115 hydrogen phthalate in the same concentration range as the samples (40-400 µM). The system blank was measured every
116 day at the beginning and the end of analyses using low-carbon Milli-Q water (<3 µM C). The instrument functioning
117 was assessed every day by comparison of data with DOC Consensus Reference Material (CRM), kindly provided by
118 Prof. D. Hansell. DOC nominal value was 41-44 µM (batch 15 Lot #07-15), DOC measured value was 42.78±1.20
119 (n=15) (Hansell, 2005).



120

121 **2.4 DOP and DON analysis**

122 Twenty-six samples out of the total 41 were analyzed for dissolved organic nitrogen (DON) and phosphorous (DOP).
123 The samples were collected between March 19th 2015 and November 3rd 2016.

124 DON was estimated by subtracting the dissolved inorganic nitrogen (DIN) from the total dissolved N (TDN). DIN and
125 TDN were analyzed by conventional, automated colorimetric procedure (CACP) according to Aminot and Kerouel
126 (2007) with an estimated limit of detection of 0.02 μM . TDN was analyzed after persulfate wet-oxidation (Pujo-Pay et
127 al., 1997).

128 DOP concentrations were determined by subtracting the inorganic form (soluble reactive phosphorus, SRP) from the
129 total dissolved P. SRP was measured spectrophotometrically after Murphy and Riley (1962) with a limit of detection of
130 0.02 μM and an analytical precision of 7% at 0.1 μM . TDP was measured as SRP after UV digestion (Armstrong et al.,
131 1966). The photooxidation technique included a 2 hours UV treatment in a Metrohm® 705 UV digester with a digestion
132 efficiency of $85 \pm 3\%$, assessed on a 1 μM solution of β -glycerol-phosphate.

133

134 **2.5 Ions and metals content in the deposition samples**

135 The concentration of soluble ions metals was measured on the samples filtered on quartz filters. These filters have low
136 blanks level for metals and ions respect to the determined concentration both in the soluble and particulate fraction. Just
137 after filtration the sample was divided in two portions, one for ionic content and the other for metal content, the latter
138 was spiked by 0.1 mL of sub-boiled distilled (s.b.) HNO_3 to preserve the metals in their soluble form.

139 Samples was keep refrigerate at $+4^\circ\text{C}$ until the analysis. Ions were determined on the solution by ion chromatography as
140 reported in Becagli et al. (2011).

141 The particulate fraction of the deposition was extracted from the quartz filter through the solubilisation procedure
142 reported in the EU EN14902 (2005) rule for aerosol samples. The extraction procedure was performed in a microwave
143 oven at 220°C for 25 min by sub-boiling distilled HNO_3 and 30% ultra-pure H_2O_2 .

144 Metals were determined in both soluble and particulate fractions by means of an Inductively Coupled Plasma Atomic
145 Emission Spectrometer (ICP-AES, Varian 720-ES) equipped with an ultrasonic nebulizer (U5000 ATC, Cetac
146 Technologies Inc.). Daily calibration standards (internal standard: 1 ppm Ge) were used for quantification.

147

148 **2.6 PM_{10} analysis**

149 PM_{10} (particulate matter with aerodynamic equivalent diameter lower than 10 μm) is routinely sampled on a daily basis
150 at the island of Lampedusa (Becagli et al., 2013; Marconi et al., 2014; Calzolari et al., 2015) by using a low-volume
151 dual-channel sequential sampler (HYDRA FAI Instruments) equipped with two PM_{10} sampling heads, operating in
152 accord with UNI EN12341. The PM_{10} mass was determined by weighting the Teflon filters (47 mm diameter 2 μm
153 nominal porosity) before and after sampling with an analytical balance in controlled conditions of temperature (20 ± 1
154 $^\circ\text{C}$) and relative humidity ($50 \pm 5\%$). The estimated error on PM_{10} mass is around 1% at $30 \mu\text{g m}^{-3}$ in the applied
155 sampling conditions. A quarter of each Teflon filter was extracted using MilliQ water (about 10 ml, accurately
156 evaluated by weighing) in ultrasonic bath for 15 min, and the ionic content was determined by ion chromatography as
157 for deposition samples (Becagli et al. 2011). Another quarter of the Teflon filter was used for the determination of
158 metals in the atmospheric particulate as already described for the deposition samples.



159

160 2.7 Enrichment factor

161 In order to obtain information on the DOM sources, DOM concentration is compared with concentration of Al, Na and
162 the enrichment factor of Pb (EF Pb) in the deposition as they are marker of crustal, sea spray and anthropic source
163 respectively.

164 The enrichment factor (EF) respect to crustal source for Pb, V and Ni are calculated by using Al as marker for crustal
165 aerosol. The following equation (Eq. 1) is used for EF calculation:

$$166 \text{ EF } X = \frac{\left(\frac{X}{Al}\right)_{\text{sample}}}{\left(\frac{X}{Al}\right)_{\text{crust}}} \quad (1)$$

167

168 where $(X/Al)_{\text{sample}}$ is the ratio between the metal X and Al concentrations in the sample, and $(X/Al)_{\text{crust}}$ is the same ratio
169 in the upper continental crust as reported in Henderson and Henderson (2009). By convention, element with $EF < 10$ are
170 called “not enriched” having a prevailing crustal source, whereas $10 < EF < 100$ indicate a moderate enrichment and
171 $EF > 100$ indicate that the element (called “enriched”) has a prevailing anthropogenic source (e.g. Lai et al., 2017).

172

173 3. Results

174 3.1 DOC atmospheric fluxes

175 DOC atmospheric fluxes ranged between 0.06 and 1.78 mmol C m⁻² day⁻¹, with a marked variability. The sampling
176 lasted for 746 days. The deposition was lower than 0.2 mmol DOC m⁻² d⁻¹ (Fig. 2 and Table 2) in half of the sampling
177 days (52%).

178 In 2015, the lowest deposition rates ($< 0.1 \text{ C m}^{-2} \text{ d}^{-1}$) were measured in July (Lmp09), October (Lmp13), and November
179 (Lmp15). The highest ones ($> 1.2 \text{ mmol C m}^{-2} \text{ d}^{-1}$) occurred between March and April (Lmp02), and in June (Lmp06),
180 both periods were characterized by dry deposition (Fig.2 and Table 2). High DOC fluxes ($> 0.6 \text{ mmol C m}^{-2} \text{ d}^{-1}$) were
181 also observed in March (Lmp01), May (Lmp04) and at the end of July (Lmp10), in correspondence with periods
182 dominated by wet deposition. In 2015, the annual rainfall was 360 mm, slightly higher than the average annual rainfall
183 at the island of Lampedusa (325 mm with 42 days of rain), (data from: <http://www.arpa.sicilia.it/> and
184 <http://www.eurometeo.com/italian/climate>).

185 In 2016, the DOC deposition rates were rather low and with a smaller variability compared to the previous year. DOC
186 fluxes ranged between 0.1 and 0.3 mmol C m⁻² d⁻¹ from January to May (Lmp18 to Lmp23), and from June to August
187 (Lmp27 to Lmp30). The highest DOC fluxes ($> 0.8 \text{ mmol C m}^{-2} \text{ d}^{-1}$) were observed in May (Lmp25) and between
188 October and November (Lmp33; Fig. 2 and Table 2).

189 In 2017, DOC fluxes ranged between 0.14 and 0.92 mmol C m⁻² d⁻¹, from January to April (Lmp36 to Lmp41); these
190 values are higher than those observed in the first three months of the previous year (Fig. 2 and Table 2).

191 Atmospheric fluxes of DOC in the wet depositions were correlated with monthly precipitation rates ($r^2=0.47$, $p < 0.05$,
192 $n=12$). The precipitation rate ranged between 2.9 and 88.5 mm.

193 A mean daily deposition of 0.33 mmol C m⁻² d⁻¹ was calculated, taking into consideration the two years (from March
194 2015 to April 2017), corresponding to an annual DOC flux of 120.7 mmol C m⁻² year⁻¹.

195

196 3.2 DON and TDN, DOP and TDP atmospheric fluxes



197 DON and Total Dissolved Nitrogen (TDN) fluxes ranged between $1.5 \cdot 10^{-3}$ and $0.25 \text{ mmol DON m}^{-2} \text{ d}^{-1}$ and between
198 $1.6 \cdot 10^{-3}$ and $0.47 \text{ mmol TDN m}^{-2} \text{ d}^{-1}$, respectively (Fig. 3 and Table 2). In most of the sampling period (93%), DON
199 deposition was lower than $0.1 \text{ mmol m}^{-2} \text{ d}^{-1}$. The main peaks were observed in March 2015 (Lmp01), in May (Lmp24
200 and Lmp25) and October 2016 (Lmp33) in correspondence with high DOC deposition (Fig. 3 and Table 2).
201 DOP and Total dissolved phosphorous (TDP) fluxes ranged between 0 and $2.7 \cdot 10^{-3} \text{ mmol DOP m}^{-2} \text{ d}^{-1}$ and $1 \cdot 10^{-4}$ and
202 $8 \cdot 10^{-5} \text{ mmol TDP m}^{-2} \text{ d}^{-1}$, respectively (Fig. 4 and Table 2). Between August 2015 and September 2016 (Lmp10-
203 Lmp30) both DOP and TDP showed low fluxes. In 2015, atmospheric DOP and TDP showed the highest fluxes in May
204 (Lmp04) and August (Lmp10). In 2016, the main peaks in DOP and TDP deposition were observed in October (Lmp31)
205 and November (Lmp33). The 4 peaks in atmospheric DOP and TDP (Lmp04, Lmp10, Lmp31 and Lmp33) were
206 responsible for 16% of total depositions and were in correspondence with high DOC fluxes (Fig. 2). It is noteworthy
207 that in March 2015 (Lmp01) and May 2016 (Lmp25), in correspondence with high fluxes of DOC, DON and TDP,
208 DOP was very low (0 and $9 \cdot 10^{-5} \text{ mmol m}^{-2} \text{ d}^{-1}$, respectively) (Table 2).
209 Taking into consideration the entire sampling period (March 2015 - November 2016), the mean DON and DOP daily
210 deposition rates were $0.032 \text{ mmol N m}^{-2} \text{ d}^{-1}$ and $3.8 \cdot 10^{-4} \text{ mmol P m}^{-2} \text{ d}^{-1}$, corresponding to an annual fluxes of 11.61
211 $\text{mmol DON m}^{-2} \text{ y}^{-1}$ and $0.14 \text{ mmol DOP m}^{-2} \text{ y}^{-1}$.
212 It should be noted that these fluxes could be underestimated due to the missing samples in 2015 and 2016.

213

214 3.3 Elemental ratios in atmospheric DOM

215 DOC:DON:DOP ratios showed a marked variability in the different periods (Fig. 5 and Table 3). DOC:DON molar
216 ratios ranged between 2.2 (Lmp24, May 2016) and 45.9 (Lmp04, May 2015) (Fig. 5a). DOC:DOP molar ratios ranged
217 between 244 (Lmp10, August 2015) and 11008 (Lmp25, May 2016) (Fig. 5b). DON:DOP ratio ranged between 9.2
218 (Lmp10, August 2015) and 1377 (Lmp25, May 2016) (Fig. 5c). No clear seasonal cycle was observed, even if in
219 autumn (November 2015 and October 2016) and late spring (May 2016) depositions were very poor in P, compared to
220 the other two elements.

221

222 3.4 The sources of atmospheric DOM

223 Previous works indicate that soluble fractions of V and Ni in aerosol samples are specific marker of anthropic source at
224 Lampedusa (Becagli et al, 2012 and 2017), but in the considered samples they usually do not show enrichment factor
225 higher than 10, therefore their source in the deposition is mainly from crustal input.

226 Besides, mean values of PM_{10} , sea salt aerosol, dust and non-sea-salt Ca (nss Ca) mean values in PM_{10} samples were
227 calculated over the same intervals of the deposition measurements.

228 In Fig. 6 we reported the DOC deposition classified on the basis of the corresponding nssCa concentration in PM_{10} .
229 Following Marconi et al. (2014), Saharan dust events are identified as those with $\text{nssCa} > 950 \text{ ng/m}^3$. DOC deposition
230 values corresponding to average nssCa larger than the threshold (950 ng/mg^3) are highlighted in red. DOC deposition
231 corresponding to a Saharan dust event occurring in at least one day of the sampling period, are indicated in orange (Fig.
232 6). A detailed description of the most interesting deposition events is given below.

233 The mean concentration of PM_{10} for Lmp01 (March 2015) was $50.1 \text{ } \mu\text{g m}^{-3}$, with an average dust value of $18.2 \text{ } \mu\text{g m}^{-3}$
234 (Table 4). This sample is dominated by crustal input as revealed by the values of nssCa in the aerosol (1327.6 ng/m^3)



235 and the Al concentration in the deposition (both soluble and particulate, Fig. 7). In this sample EF(Pb) indicate the low
236 contribution of the anthropic source. Na concentration in the deposition is $304 \text{ mg m}^{-2} \text{ d}^{-1}$ (Fig. 7).
237 Lmp02 (March-April 2015) is characterized by the second highest DOC deposition, even if no Saharan dust event
238 occurred in this period (Fig. 6 and 7). PM_{10} mean concentration was $29 \mu\text{g m}^{-3}$, the average sea-salt aerosol value was
239 $13.6 \mu\text{g m}^{-3}$ (Table 4), with a contribution to PM_{10} of 47%. This sample is strongly affected by sea spray as indicated by
240 the Na/Al ratio that is 60-fold higher than in Lmp01, even if the concentration of Na in the deposition is slightly low
241 than in Lmp01.
242 Lmp04 (May 2015) shows a high value of DOC; during this sampling period a Saharan dust event occurred (Fig. 6), but
243 the concentration of Al in the deposition was quite low (Fig. 7). The PM_{10} mean concentration was $26.4 \mu\text{g m}^{-3}$ and the
244 average sea-salt in the aerosol was 8.8 g m^{-3} , contributing by one third to the total particulate matter. As for Lmp03 the
245 ratio Na/Al is quite high suggesting that sea spray dominates also in this sample.
246 The mean PM_{10} concentration of Lmp06 (June 2015), was $23.3 \mu\text{g m}^{-3}$, with an average sea-salt aerosol concentration of
247 $13.6 \mu\text{g m}^{-3}$ (Table 4). The average contribution of sea salt aerosol to the particulate matter concentration was 27%. The
248 peculiar characteristic of this sample is the high concentration of soluble Al and low particulate Al in the deposition
249 (Fig. 7). This feature is also observed in the samples Lmp10 and Lmp12 presenting quite high concentration of DOC in
250 July and September 2015.
251 Lmp25 (May 2016) was characterized by a mean PM_{10} concentration of $133.7 \mu\text{g m}^{-3}$ with a peak of $267.4 \mu\text{g m}^{-3}$, and
252 with an average dust value of $42.5 \mu\text{g m}^{-3}$ (Table 4). This is the highest value of PM_{10} observed in the entire sampling
253 period and indicates the occurrence of a Saharan dust event. The average value of nssCa in the sampling days was
254 4815.1 ng/m^3 , with an incredible peak of 9207 ng/m^3 , highlighting the occurrence of an intense Saharan dust event. The
255 relevant Saharan dust contribution for this sample is well revealed by Al concentration (both soluble and particulate) in
256 the atmospheric deposition (Fig. 7).
257 Lmp33 (October-November 2016) and Lmp34 (November 2016) present a very indicative pattern of the two possible
258 source of DOC, crustal and sea spray. Lmp33 shows higher DOC concentration than Lmp34. The former is
259 characterized by very high Na concentration in the deposition, conversely the second is characterized by high crustal
260 content (as revealed by the high concentration of Al, Fig. 7).
261 Unfortunately PM_{10} data are not available for the fourth highest DOC deposition of the entire study period (Lmp37).

262

263 4. Discussion

264 4.1 DOC input from the atmosphere

265 The relationship between monthly precipitation rates and DOC fluxes confirmed the high efficiency in DOM
266 atmospheric deposition of DOC via rain events in the Med Sea, as recently reported by Djaoudi et al. (2018).
267 Our data allowed for the quantification of the DOC annual input from the atmosphere ($120.7 \text{ mmol C m}^{-2} \text{ y}^{-1}$); this value
268 is very close to that measured at Cap Ferrat peninsula (Southern France) in 2006 ($129 \text{ mmol C m}^{-2} \text{ y}^{-1}$; Pulido-Villena et
269 al., 2008) and in three lakes in the western Mediterranean basin (Southern Spain, $153.3 \text{ mmol C m}^{-2} \text{ y}^{-1}$ in 2005; De
270 Vicente et al., 2012). This value is higher than that reported for the north-western Med Sea from February 2015 to July
271 2016, at Frioul island, Marseille Bay ($59 \text{ mmol C m}^{-2} \text{ y}^{-1}$; Djaoudi et al., 2018). If the same sampling period is taken
272 into consideration for both studies (from March 2015, the beginning of sampling in Lampedusa, to July 2016, the end of
273 sampling at Frioul island), DOC input is 2-times higher at Lampedusa than at Frioul Island. This variability is probably



274 due to the different temporal and seasonal cycles of dry and wet deposition. In particular the marked differences
275 between these two sites could be influenced by the presence of a south-north decreasing gradient in the intensity of the
276 mineral dust deposition as proposed by Vincent et al. (2016). Our data also show high variability in DOC deposition
277 rates without a clear seasonality. If in 2015 and 2016 the highest deposition rates were between spring and autumn, in
278 2017 the highest deposition rates were in winter. In addition the two highest peaks observed in 2015 (Lmp02 and
279 Lmp06, dry deposition) together accounted for 43% of the annual DOC flux ($52 \text{ mmol C m}^{-2} \text{ y}^{-1}$). Depending on the
280 origin and trajectories of the air masses, atmosphere can carry significant amounts of DOC.

281 Assuming that the annual DOC flux from this study ($120.7 \text{ mmol C m}^{-2} \text{ y}^{-1}$) is valid for the whole Med Sea
282 (area= $2.5 \cdot 10^{12} \text{ m}^2$), we can estimate a total input of $3.64 \text{ Tg DOC y}^{-1}$. The global estimation for wet atmospheric DOC
283 deposition is $306\text{-}580 \text{ Tg C y}^{-1}$ and the input to the global ocean ranges between 90 and 246 Tg C y^{-1} (Willey et al.,
284 2000; Kanakidou et al., 2012). The global dry deposition of OC has been estimated to be 11 Tg C y^{-1} , (Jurado et al.,
285 2008) leading to a total OC deposition to the oceans of $101\text{-}247 \text{ Tg C y}^{-1}$. The comparison of these estimates indicates
286 that the Med Sea receives from 1.5 to 4% of the global atmospheric input of DOC, despite it covers only 0.7% of the
287 global oceans area.

288 Moreover, if we consider the riverine DOC fluxes, our values are up to 6 times larger than the estimate of the total river
289 input to the Med Sea ($0.6\text{-}0.7 \text{ Tg DOC y}^{-1}$; Santinelli, 2015). These results confirm the lead role of atmosphere in the
290 transport of allochthonous DOC to the Med Sea, as suggested recently by Galletti et al. (2019).

291 Few episodes of Saharan outbreaks can strongly affect the annual dust flux, indeed a single outbreak can account for
292 40-80% of the flux (Guerzoni et al., 1997). The most intense dust deposition events in Lampedusa generally display
293 larger values in spring (March-June) and in autumn (Vincent et al., 2016; Bergametti et al., 1989; Loye-Pilot and
294 Martin, 1996; Avila et al., 1997; TERNON et al., 2010). Deposition data in this work reveal that dust events can contribute
295 to the annual DOC fluxes but sea spray seems the dominant source of DOC in this area.

296 It should also be stressed that the DOC dynamics and its annual fluxes are not only influenced by dust deposition
297 events. The wet deposition is also relevant, and the correlation between monthly precipitation rates and DOC fluxes
298 confirms the high efficiency in DOC atmospheric deposition via rain events in the Med Sea, as recently proposed by
299 Djaoudi et al. (2018).

300

301 **4.2 Atmospheric DON, DOP input and elemental ratios**

302 The DON annual flux ($11.61 \text{ mmol N m}^{-2} \text{ y}^{-1}$), observed at Lampedusa, was lower than that measured at Frioul Island
303 ($17.80 \text{ mmol N m}^{-2} \text{ y}^{-1}$; Djaoudi et al., 2018). Only the study by Markaki et al. (2010) reports data on atmospheric DON
304 fluxes and is focused on the Eastern Med Sea. These authors reported an annual flux ($18.49 \text{ mmol N m}^{-2} \text{ y}^{-1}$) higher than
305 that observed at Lampedusa. The comparison among our values ($0.14 \text{ mmol P m}^{-2} \text{ y}^{-1}$) and the few DOP data reported in
306 the literature shows that the fluxes at Lampedusa are markedly higher than those reported for the Western Med Sea
307 ($0.07 \text{ mmol P m}^{-2} \text{ y}^{-1}$, Djaoudi et al., 2018; $0.03 \text{ mmol P m}^{-2} \text{ y}^{-1}$, Migon and Sandroni, 1999), whereas they are lower
308 than those obtained by Violaki et al. (2017) for both the West ($1.16 \text{ mmol P m}^{-2} \text{ y}^{-1}$) and East ($0.90 \text{ mmol P m}^{-2} \text{ y}^{-1}$) Med
309 Sea. Our values are instead very similar to those reported for the Eastern Med Sea in 2001 and 2002 ($0.15 \text{ mmol P m}^{-2}$
310 y^{-1}) (Markaki et al., 2010).

311 Over the entire time-series, the average DOP and DON contributions to TDP and TDN were 40% and 26%,
312 respectively. These data confirm that a significant fraction of the dissolved P and N in the atmospheric deposition was



313 in the organic form. These values are similar to those observed in previous studies at Frioul Island (DOP 40%, DON
314 25%; Djaoudi et al., 2018), and in both the western and eastern Med Sea (DOP 38%; DON 32%; Markaki et al., 2010).
315 The similarity among the depositions collected at the two sites (Lampedusa, Central Med Sea and Frioul, North-western
316 Med Sea) suggests that the remote site of Lampedusa may be representative of what the Mediterranean area receives in
317 terms of DON and DOP, especially in the western basin.

318 The data on atmospheric elemental ratios show that each deposition event is characterized by a specific elemental ratio,
319 suggesting a high variability in DOM composition and the presence of multiple sources. Djaoudi et al (2018) observed
320 an average value of DOC:DON:DOP molar ratios of 1228:308:1 in atmospheric DOM, collected in the north-western
321 Med Sea. In the surface Med Sea, DOC:DON:DOP ratios ranges between 1050:84:1 in the western basin to 1560:120:1
322 in the eastern basin (Pujo-Pay et al., 2011). The average values observed in our atmospheric deposition time-series
323 (1909:292:1) indicate that atmospheric DOM is enriched in DOC and DON with respect to marine DOM. This
324 observation is also valid when we compare our values with those recently measured on marine samples collected at the
325 MOOSE ANTARES offshore station (north-western Med Sea) (1227:100:1, Djaoudi et al., 2018).

326

327 **4.3 The contribution of Saharan dust to atmospheric fluxes of dissolved organic carbon**

328 The input of Saharan dust has important effects on the chemistry of the Mediterranean aerosols and its deposition can
329 enrich the Med Sea with many elements (such as Co, Ni, trace metals). Very few data are available on the interactions
330 between organic carbon and Saharan dust, even if organic material found in the troposphere is often associated with
331 dust particles (Usher et al., 2003; Aymoz et al., 2004).

332 Our results show that Saharan dust events can represent a relevant, albeit intermittent, source of DOC to the central Med
333 Sea. Focusing on the different peaks of DOC deposition, our results indicate that Lmp01, Lmp04 and Lmp25 are
334 associated to a Saharan dust event and that the aerosol, during its route to Lampedusa, was probably enriched with
335 organic substances. We hypothesize that the dust particles present in the aerosol worked as condensation nuclei for
336 organic molecules, facilitating their accumulation and transport (Usher et al., 2003). The role of Saharan dust in the
337 transport of DOC is evident in Lmp25 (May 2016) characterized by high DOC, when an intense intrusion of Saharan air
338 masses was favored by one synoptic situation in which the role of the cyclonic circulation with a minimum depression
339 was significant (www.meteogiornale.it).

340 If all the Saharan dust deposition events (red and orange in Fig. 6) are taken into account, the input of 49.58 mmol
341 DOC m⁻² to Lampedusa during the study period can be estimated, this value represents ~41% of the total flux for the
342 entire sampling period. Instead, if only the strong dust events (red in Fig. 6) are taken into consideration a flux of 15.26
343 mmol DOC m⁻² can be estimated, representing 13% of the total flux. Anyhow each deposition event must be considered
344 individually, because it can be characterized by an enrichment of DOC or not depending on the aerosol load (Formenti
345 et al., 2003; Aymoz et al., 2004).

346 Wet deposition mainly controls the flux of Saharan dust to the Med Sea, but dry deposition can be also important
347 (Guerzoni et al., 1997) and its relative importance strongly depends on meteorological conditions and local emission
348 (Inomata et al., 2009). Some models have estimated that wet deposition represents up to 75-95% of total deposition
349 (Iavorivska et al., 2016). Our data confirm the importance of wet deposition, but similarly dry deposition also plays a
350 crucial role. Our results stress the relevance of dry deposition (32% of the total deposition during the entire sampling



351 period) that, in the remote site of Lampedusa, appears to be main contributor of DOC and of other chemical species, as
352 suggested in the past by Morales-Baquero et al. (2013).
353 It is also evident by our data that Saharan dust input is not always associated with high DOC input, it cannot therefore
354 be considered as the only process for DOC transport and deposition. For instance sample Lmp34, that shows high
355 concentration of dust, is not characterized by high concentration of DOC and several samples (for example Lmp02,
356 Lmp33 and Lmp37) characterized by high concentration of DOC, do not show high crustal content. Indeed high DOC
357 deposition seems often associated to sea spray transport, for instance in samples Lmp02, Lmp10, Lmp 12, Lmp 33 and
358 Lmp 37 (Fig. 6, in gray).
359 Lmp23, Lmp27, Lmp32, Lmp35 and Lmp36 were not characterized by high DOC fluxes (Fig. 6), even if these
360 sampling periods were characterized by at least a strong Saharan dust event (Fig. 6, in orange). This observation
361 supports the hypothesis that dust from Saharan region is not typically enriched with DOC, but it behaves as aggregation
362 center of organic molecules in the atmosphere, and depending on its route it can be enriched or not in DOC during its
363 route. Lmp34 further supports this hypothesis. This sample shows the third highest average nss Ca value (1092.2
364 ng/m^3), nevertheless DOC was very low ($0.20 \text{ mmol m}^{-2} \text{ d}^{-1}$), below the daily average flux of the entire sampling period
365 ($0.33 \text{ mmol m}^{-2} \text{ d}^{-1}$) (Fig. 6, Tables 2 and 4).
366 However the data of atmospheric Na and soluble Al suggest a very high contribution of sea spray aerosol (the highest of
367 the whole considered period) (Fig. 7). Therefore, for samples Lmp33 and Lmp37 the DOC source seems to be primary
368 marine instead of crustal as for the samples Lmp01, Lmp04, Lmp10, Lmp12 and especially Lmp25.
369 Lastly, it is interesting to notice that samples characterized by high values of DOC never present high EF(Pb) and the
370 samples presenting $\text{EF(Pb)} > 10$ present very low DOC concentration, suggesting that anthropic sources have a small
371 impact on DOC deposition at Lampedusa.

372

373 **4.4 Implications for marine ecosystem**

374 The measurements carried out at the Island of Lampedusa clearly show that the atmosphere is an important source of
375 allochthonous DOC to the Central Med Sea. Very few information is available about the biological lability of
376 atmospheric DOC: if labile, it can be used very quickly by the microbial loop, whereas if it is mainly recalcitrant, it can
377 accumulate and be transported by water masses circulation.

378 In order to estimate the impact of atmospheric DOC deposition to the surface waters we took into consideration a mixed
379 layer depth (MLD) ranging between 15 and 30 m, typical of the sea close to the island of Lampedusa in September, in
380 according with the estimation reported by D'Ortenzio et al. (2005). Santinelli et al. (2012) observed an average DOC
381 concentration of $60 \mu\text{M}$ in the same area in September 1999 (in the mixed layer), and estimated a bacterial carbon
382 demand (BCD) of $0.32 \mu\text{M C d}^{-1}$ (assuming a bacterial growth efficiency of 15%), which represents the total amount of
383 carbon needed to support the observed bacterial production. In September, the atmospheric DOC flux was 0.24 mmol C
384 $\text{m}^{-2} \text{ d}^{-1}$ in 2015 and $0.38 \text{ C m}^{-2} \text{ d}^{-1}$ in 2016, dividing them by the average MLD (22.5 m) (D'Ortenzio et al. 2005), we
385 estimate that the atmospheric input is expected to determine a $0.011\text{-}0.017 \mu\text{M DOC d}^{-1}$ increase in the mixed layer.
386 Assuming that the values of BCD observed in September 1999 ($0.32 \mu\text{M C d}^{-1}$) are valid also for September 2015 and
387 2016, and that all the DOC coming from the atmosphere is labile, it could satisfy 3-5% of the daily BCD. Instead in
388 summer the MLD is between 10 and 15 m, with an average value of 12.5 m (D'Ortenzio et al. 2005). The DOC input
389 from the atmosphere is expected to increase the DOC concentration in the mixed layer by $0.008\text{-}0.079 \mu\text{M C d}^{-1}$ from



390 June to August 2015, and by 0.013-0.014 from June to August 2016. Assuming that a BCD of $0.32 \mu\text{M C d}^{-1}$ is valid
391 also for summer (three months) and that all the atmospheric DOC is labile, it could satisfy 3-25% of the daily BCD.
392 These results highlight the relevant role of atmosphere input of DOC in sustaining the bacterial productivity in the
393 surface layer, particularly when the column is strongly stratified.
394 The Mediterranean MLD seasonal variability is characterized by a basin scale deepening from November to February-
395 March and an abrupt stratification in April, which is maintained throughout the summer and early autumn. Even if these
396 data stress the potential role of atmospheric DOC in sustaining bacterial productivity in the surface ocean, a time series
397 of BCD, MLD and DOC concentrations in the surface layer are crucial in order to have an accurate estimation of the
398 DOC atmospheric input impact on the functioning of marine ecosystem. It should be also noted that a fraction of
399 atmospheric DOC could be recalcitrant, and therefore could be transported to depth, playing a key role in carbon
400 sequestration to depth. The refractory nature of a part of atmospheric DOC is hypothesized by Sánchez-Pérez et al.
401 (2016), who collected a 2-year time series data on Fluorescent DOM (FDOM) deposition in the North-western Med Sea
402 and studied the changes in the quality and quantity of marine DOM in the Barcelona coastal area (Spain). Their results
403 show that atmospheric inputs induced changes in the quality of organic matter, increasing the proportion of FDOM
404 substances in DOM pool.
405 Lastly, as highlighted in the previous paragraphs, the occurrence of Saharan dust events opens interesting considerations
406 on their impact on the marine environment. Previous studies suggested that dust inputs can promote autotrophic
407 production (Ridame and Guieu, 2002; Markaki et al., 2003). Instead Pulido-Villena et al. (2008) experimentally found
408 that heterotrophic bacteria can reduce the amount of C exported to deeper waters, because a Saharan dust event would
409 have induced the mineralization of 22-70% of bioavailable DOC, changing carbon sequestration.

410

411 **4. Conclusions**

412 Our data show that atmospheric input has a larger impact to the Med Sea than to the global ocean and DOC fluxes from
413 the atmosphere to the Med Sea can be up to 6-fold larger than river input.

414 This study indicates that the organic substances transported by Saharan dust at Lampedusa site mainly have natural
415 origin, especially from sea spray and that Saharan dust can be an important carrier of organic substances. The load of
416 DOC associated with dust is very variable and high DOC fluxes were observed also in absence of dust deposition
417 events.

418 Atmospheric C:N:P molar ratios indicate that DOM is enriched in DOC and DON with respect to marine DOM and that
419 the contribution of atmospheric deposition to the marine DOM stoichiometry in the Med Sea could be relevant, in
420 particular during the stratification period.

421 For future studies, atmospheric and marine DOM molar ratios (C:N:P) could be measured over time in order to obtain
422 information about changes in marine DOM pool. Further studies are needed to understand the link between atmospheric
423 inputs and marine biogeochemistry. Data on stable carbon ($\delta^{13}\text{C}$) on atmospheric DOC would be crucial in order to gain
424 information about its main sources. Incubation experiments should be carried out, both with aerosol rich or poor in
425 DOC, in order to better understand how the microbial community can respond to dust input. Lastly, longer time series,
426 combined with a modelling effort, are highly desirable in order to assess the response of DOM dynamics in the Med Sea
427 to the change in aerosol deposition pattern due to the effect of climate change.



428 **Author contribution**

429 YG and CS conceived of the study and the sampling design. YG, SB, DMS collected the samples. YG, MG, SB, RT,
430 SV analyzed the samples. YG, CS, EPV, AdS analyzed the data and all authors assisted with data discussion and
431 contributed to the revision and editing of the final manuscript. All authors are aware of and accept responsibility for this
432 manuscript and have approved the final submitted manuscript.

433

434 **Acknowledgements**

435 Part of this research was supported by “Professionalità” project, funded by the *Fondazione Banca del Monte di*
436 *Lombardia*. The authors thank the analytical platform PACEM (Mediterranean Institute of Oceanography) for the
437 analysis of organic and inorganic forms of nitrogen.

438

439 *The authors declare that they have no conflict of interest.*

440

441 *The dataset generated for this study are available on request to the corresponding author.*

442

443 **References**

- 444 Armstrong, F. A. J., Williams, P. M., and Strickland, J. H.: Photo-oxidation of organic matter in sea water by ultra-
445 violet radiation, analytical and other applications, *Nature*, 211(5048), 481, <https://doi.org/10.1038/211481a0>,
446 1966.
- 447 Aminot, A., and K erouel, R.: *Dosage automatique des nutriments dans les eaux marines: m ethodes en flux continu*,
448 Editions Quae, 2007.
- 449 Aymoz, G., Jaffrezo, J. L., Jacob, V., Colomb, A., and George, C.: Evolution of organic and inorganic components of
450 aerosol during a Saharan dust episode observed in the French Alps, *Atmospheric Chemistry and Physics*,
451 4(11/12), 2499-2512, <https://doi.org/10.5194/acp-4-2499-2004>, 2004.
- 452 Avila, A., Queralt-Mitjans, I., and Alarc on, M. : Mineralogical composition of African dust delivered by red rains over
453 northeastern Spain. *Journal of Geophysical Research: Atmospheres*, 102(D18), 21977-21996,
454 <https://doi.org/10.1029/97JD00485>, 1997.
- 455 Becagli, S., Ghedini, C., Peeters, S., Rottiers, A., Traversi, R., Udisti, R., Chiari, M., Jalba, A., Despiu, S., Dayan, U.,
456 and Temara, A.: MBAS (Methylene Blue Active Substances) and LAS (Linear Alkylbenzene Sulphonates) in
457 Mediterranean coastal aerosols: sources and transport processes, *Atmospheric environment*, 45(37), 6788-6801,
458 <https://doi.org/10.1016/j.atmosenv.2011.04.041>, 2011.
- 459 Becagli, S., Sferlazzo, D. M., Pace, G., di Sarra, A., Bommarito, C., Calzolari, G., Ghedini, C., Lucarelli, F., Meloni, D.,
460 Monteleone, F., Severi, M., Traversi, R., and Udisti, R.: Evidence for heavy fuel oil combustion aerosols from
461 chemical analyses at the island of Lampedusa: a possible large role of ships emissions in the Mediterranean,
462 *Atmospheric Chemistry and Physics*, 12(7), 3479-3492, <https://doi.org/10.5194/acp-12-3479-2012>, 2012.
- 463 Becagli, S., Lazzara, L., Fani, F., Marchese, C., Traversi, R., Severi, M., di Sarra, A., Sferlazzo, D. M., Piacentino, S.,
464 Bommarito, C., Dayan, U., and Udisti, R.: Relationship between methanesulfonate (MS⁻) in atmospheric
465 particulate and remotely sensed phytoplankton activity in oligo-mesotrophic central Mediterranean Sea,
466 *Atmospheric Environment*, 79, 681-688, <https://doi.org/10.1016/j.atmosenv.2013.07.032>, 2013.
- 467 Becagli, S., Anello, F., Bommarito, C., Cassola, F., Calzolari, G., Iorio, T. D., di Sarra, A., G omez-Amo, J. -L.,
468 Lucarelli, F., Marconi, M., Meloni, D., Monteleone, F., Nava, S., Pace, G., Severi, M., Sferlazzo, D. M.,
469 Traversi, R., and Udisti, R.: Constraining the ship contribution to the aerosol of the central Mediterranean,
470 *Atmospheric Chemistry and Physics*, 17(3), 2067-2084, <https://doi.org/10.5194/acp-17-2067-2017>, 2017.
- 471 Bergametti, G., Dutot, A. L., Buat-Menard, P., Losno, R., and Remoudaki, E.: Seasonal variability of the elemental
472 composition of atmospheric aerosol particles over the northwestern Mediterranean, *Tellus B*, 41(3), 353-361,
473 <https://doi.org/10.1111/j.1600-0889.1989.tb00314.x>, 1989.
- 474 Calzolari, G., Nava, S., Lucarelli, F., Chiari, M., Giannoni, M., Becagli, S., Traversi, R., Marconi, M., Frosini, D.,
475 Severi, M., Udisti, R., di Sarra, A., Pace, G., Meloni, D., Bommarito, C., Monteleone, F., Anello, F., and
476 Sferlazzo, D. M.: Characterization of PM 10 sources in the central Mediterranean, *Atmospheric Chemistry and*
477 *Physics*, 15(24), 13939-13955, <https://doi.org/10.5194/acp-15-13939-2015>, 2015.



- 478 D'Ortenzio, F., Iudicone, D., de Boyer Montegut, C., Testor, P., Antoine, D., Marullo, S., Santoleri, R., and Madec, G.:
479 Seasonal variability of the mixed layer depth in the Mediterranean Sea as derived from in situ profiles,
480 Geophysical Research Letters, 32(12), <https://doi.org/10.1029/2005GL022463>, 2005.
- 481 De Vicente, I., Ortega-Retuerta, E., Morales-Baquero, R., and Reche, I.: Contribution of dust inputs to dissolved
482 organic carbon and water transparency in Mediterranean reservoirs, Biogeosciences 9, 5049-5060,
483 <https://doi.org/10.5194/bg-9-5049-2012>, 2012.
- 484 Djaoudi, K., Van Wambeke, F., Barani, A., Hélias-Nunige, S., Sempéré, R., and Pulido-Villena, E.: Atmospheric fluxes
485 of soluble organic C, N, and P to the Mediterranean Sea: Potential biogeochemical implications in the surface
486 layer, Progress in Oceanography, 163, 59-69, <https://doi.org/10.1016/j.pocean.2017.07.008>, 2018.
- 487 Economou, C., and Mihalopoulos, N.: Formaldehyde in the rainwater in the eastern Mediterranean: occurrence,
488 deposition and contribution to organic carbon budget, Atmospheric Environment 36(8), 1337-1347,
489 [https://doi.org/10.1016/S1352-2310\(01\)00555-6](https://doi.org/10.1016/S1352-2310(01)00555-6), 2002.
- 490 Formenti, P., Elbert, W., Maenhaut, W., Haywood, J., Osborne, S., and Andreae, M. O.: Inorganic and carbonaceous
491 aerosols during the Southern African Regional Science Initiative (SAFARI 2000) experiment: Chemical
492 characteristics, physical properties, and emission data for smoke from African biomass burning, Journal of
493 Geophysical Research: Atmospheres, 108(D13), <https://doi.org/10.1029/2002JD002408>, 2003.
- 494 Galletti, Y., Gonnelli, M., Retelletti Brogi, S., Vestri, S., and Santinelli, C.: DOM dynamics in open waters of the
495 Mediterranean Sea: New insights from optical properties, Deep Sea Research Part I: Oceanographic Research
496 Papers, 144, 95-114, <https://doi.org/10.1016/j.dsr.2019.01.007>, 2019.
- 497 Goudie, A. S., and Middleton, N. J.: Saharan dust storms: nature and consequences, Earth-science reviews, 56(1-4),
498 179-204, [https://doi.org/10.1016/S0012-8252\(01\)00067-8](https://doi.org/10.1016/S0012-8252(01)00067-8), 2001.
- 499 Guerzoni, S., and Chester, R. (Eds.): The impact of desert dust across the Mediterranean (Vol. 11), Springer Science &
500 Business Media, Netherlands, 1996.
- 501 Guerzoni, S., Molinaroli, E., and Chester, R.: Saharan dust inputs to the western Mediterranean Sea: depositional
502 patterns, geochemistry and sedimentological implications, Deep Sea Research Part II: Topical Studies in
503 Oceanography, 44(3), 631-654, [https://doi.org/10.1016/S0967-0645\(96\)00096-3](https://doi.org/10.1016/S0967-0645(96)00096-3), 1997.
- 504 Henderson, P., and Henderson, G.M. (Eds.): The Cambridge Handbook of Earth Science Data. University Press,
505 Cambridge, 2009.
- 506 Hansell, D.A.: Dissolved organic carbon reference material program. Eos, Transactions American Geophysical Union
507 86(35), 318-318, <https://doi.org/10.1029/2005EO350003>, 2005.
- 508 Herut B., Collier R., and Krom M.D.: The role of dust in supplying nitrogen and phosphorus to the South East
509 Mediterranean. Limnology and Oceanography, 47:870-878, <https://doi.org/10.4319/lo.2002.47.3.0870>, 2002.
- 510 Iavorivska, L., Boyer, E. W., and DeWalle, D. R.: Atmospheric deposition of organic carbon via precipitation,
511 Atmospheric Environment, 146, 153-163, <https://doi.org/10.1016/j.atmosenv.2016.06.006>, 2016.
- 512 Inomata, Y., Igarashi, Y., Chiba, M., Shinoda, Y., and Takahashi, H.: Dry and wet deposition of water-insoluble dust
513 and water-soluble chemical species during spring 2007 in Tsukuba, Japan, Atmospheric Environment, 43(29),
514 4503-4512, <https://doi.org/10.1016/j.atmosenv.2009.06.048>, 2009.
- 515 IPCC (Eds.): Climate change: mitigation of climate change, In: Edenhofer, O., Pichs-Madruga, R., Sokona, Y.,
516 Farahani, E., Kadner, S., Seyboth, K., Adler, A., Baum, I., Brunner, S., Eickemeier, P., Kriemann, B.,
517 Savolainen, J., Schlömer, S., von Stechow, C., Zwickel, T., and Minx, J. C., Contribution of working group III to
518 the fifth assessment report of the intergovernmental panel on climate change, Cambridge University Press,
519 Cambridge, 2014.
- 520 Jurado, E., Dachs, J., Duarte, C. M., and Simo, R.: Atmospheric deposition of organic and black carbon to the global
521 oceans, Atmospheric Environment, 42(34), 7931-7939, <https://doi.org/10.1016/j.atmosenv.2008.07.029>, 2008.
- 522 Kanakidou, M., Duce, R. A., Prospero, J. M., Baker, A. R., Benitez-Nelson, C., Dentener, F. J., Hunter, K. A., Liss, P.
523 S., Mahowald, N., Okin, G. S., Sarin, M., Tsigaridis, K., Uematsu, M., Zamora, L. M., and Zhu, T.: Atmospheric
524 fluxes of organic N and P to the global ocean, Global Biogeochemical Cycles 26(3),
525 <https://doi.org/10.1029/2011GB004277>, 2012.
- 526 Lai, A. M., Shafer, M. M., Dibb, J. E., Polashenski, C. M., and Schauer, J. J.: Elements and inorganic ions as source
527 tracers in recent Greenland snow, Atmospheric Environment, 164, 205-215, 2017.
- 528 Loÿe-Pilot, M. D., and Martin, J. M. (Eds.): Saharan dust input to the western Mediterranean: an eleven years record in
529 Corsica, In The impact of desert dust across the Mediterranean (pp. 191-199), Springer, Dordrecht, 1996.
- 530 Marconi, M., Sferlazzo, D. M., Becagli, S., Bommarito, C., Calzolari, G., Chiari, M., di Sarra, A., Ghedini, C.,
531 Gómez-Amo, J. L., Lucarelli, F., Meloni, D., Monteleone, F., Nava, S., Pace, G., Piacentino, S., Rugi, F.,
532 Severi, M., Traversi, R., and Udisti, R.: Saharan dust aerosol over the central Mediterranean Sea: PM10
533 chemical composition and concentration versus optical columnar measurements, Atmos. Chem. Phys., 14,
534 2039-2054, <https://doi.org/10.5194/acp-14-2039-2014>, 2014.
- 535 Markaki, Z., Oikonomou, K., Kocak, M., Kouvarakis, G., Chaniotaki, A., Kubilay, N., and Mihalopoulos, N.:
536 Atmospheric deposition of inorganic phosphorus in the Levantine Basin, eastern Mediterranean: Spatial and

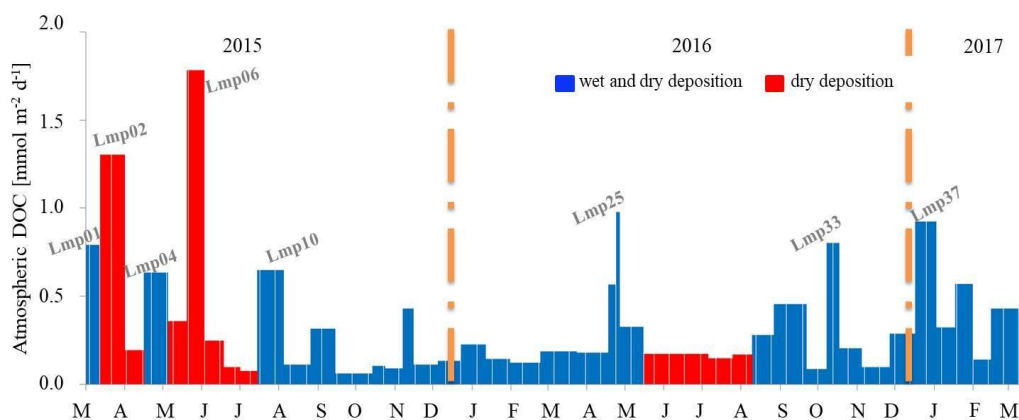


- 537 temporal variability and its role in seawater productivity, *Limnology and Oceanography*, 48(4), 1557-1568,
538 <https://doi.org/10.4319/lo.2003.48.4.1557>, 2003.
- 539 Markaki, Z., Lojze-Pilot, M. D., Violaki, K., Benyahya, L., and Mihalopoulos, N.: Variability of atmospheric deposition
540 of dissolved nitrogen and phosphorus in the Mediterranean and possible link to the anomalous seawater N/P
541 ratio, *Marine Chemistry*, 120(1-4), 187-194, <https://doi.org/10.1016/j.marchem.2008.10.005>, 2010.
- 542 Mermex group (Eds.): White book of Mermex program, *Progress in Oceanography*, 91, 97-166,
543 <https://doi.org/10.1016/j.pocean.2011.02.003>, 2011.
- 544 Migon, C., Copin-Montegut, G., Elegant, L., and Morelli, J.: Atmospheric input of nutrients to the coastal
545 Mediterranean area, *Biogeochemical implications*, *Oceanologica acta*. Paris, 12(2), 187-191, 1989.
- 546 Migon, C., and Sandroni, V.: Phosphorus in rainwater: Partitioning inputs and impact on the surface coastal ocean,
547 *Limnology and Oceanography*, 44(4), 1160-1165, <https://doi.org/10.4319/lo.1999.44.4.1160>, 1999.
- 548 Morales-Baquero, R., Pulido-Villena, E., and Reche, I.: Chemical signature of Saharan dust on dry and wet atmospheric
549 deposition in the south-western Mediterranean region, *Tellus B: Chemical and Physical Meteorology*, 65(1),
550 18720, <https://doi.org/10.3402/tellusb.v65i0.18720>, 2013.
- 551 Murphy, J., and Riley, J. P.: A modified single solution method for the determination of phosphate in natural water,
552 *Analytica chimica acta*, 27, 31-36, [https://doi.org/10.1016/S0003-2670\(00\)88444-5](https://doi.org/10.1016/S0003-2670(00)88444-5), 1962.
- 553 Pace, G., Meloni, D., and di Sarra, A.: Forest fire aerosol over the Mediterranean basin during summer 2003, *Journal*
554 *Geophys. Res.*, 110, D21202, <https://doi.org/doi:10.1029/2005JD005986>, 2005.
- 555 Pace, G., di Sarra, A., Meloni, D., Piacentino, S., and Chamard, P.: Optical properties of aerosols over the central
556 Mediterranean, 1. Influence of transport and identification of different aerosol types, *Atmos. Chem. Phys.*, 6,
557 697-713, 2006.
- 558 Prospero, J. M., Blades, E., Mathison, G., and Naidu, R.: Interhemispheric transport of viable fungi and bacteria from
559 Africa to the Caribbean with soil dust, *Aerobiologia*, 21(1), 1-19, <https://doi.org/10.1007/s10453-004-5872-7>,
560 2005.
- 561 Pulido-Villena, E., Wagener, T., and Guieu, C.: Bacterial response to dust pulses in the western Mediterranean:
562 Implications for carbon cycling in the oligotrophic ocean, *Global Biogeochemical Cycles*, 22(1),
563 <https://doi.org/10.1029/2007GB003091>, 2008.
- 564 Pujo-Pay, M., Conan, P., and Raimbault, P.: Excretion of dissolved organic nitrogen by phytoplankton assessed by wet
565 oxidation and ¹⁵N tracer procedures, *Marine Ecology Progress Series*, 153, 99-111,
566 <https://doi.org/10.3354/meps153099>, 1997.
- 567 Pujo-Pay, M., Conan, P., Oriol, L., Cornet-Barthaux, V., Falco, C., Ghiglione, J. F., Goyet, C., Moutin T., and Prieur,
568 L.: Integrated survey of elemental stoichiometry (C, N, P) from the western to eastern Mediterranean Sea, 2011.
- 569 Ridame, C., and Guieu, C.: Saharan input of phosphate to the oligotrophic water of the open western Mediterranean
570 Sea, *Limnology and Oceanography*, 47(3), 856-869, <https://doi.org/10.4319/lo.2002.47.3.0856>, 2002.
- 571 Sánchez-Pérez, E. D., Marín, I., Nunes, S., Fernández-González, L., Peters, F., Pujo-Pay, M., Conan, P., Marrasé, C.:
572 Aerosol inputs affect the optical signatures of dissolved organic matter in NW Mediterranean coastal waters,
573 *Scientia Marina* 80(4), 437-446, <https://doi.org/10.3989/scimar.04318.20B>, 2016.
- 574 Santinelli, C., Sempéré, R., Van Wambeke, F., Charriere, B., and Seritti, A.: Organic carbon dynamics in the
575 Mediterranean Sea: An integrated study, *Global Biogeochemical Cycles*, 26(4), 2012.
- 576 Santinelli, C.: DOC in the Mediterranean Sea. In: Hansell D.A., Carlson C.A. (Eds.), *Biogeochemistry of Marine*
577 *Dissolved Organic Matter* (Second edition), Academic Press, San Diego, pp. 579-608,
578 <https://doi.org/10.1016/B978-0-12-405940-5.00013-3>, 2015.
- 579 Sellitto, P., Zanetel, C., di Sarra, A., Salerno, G., Tapparo, A., Meloni, D., Pace, G., Caltabiano, T., Briole, P., and
580 Legras, B.: The impact of Mount Etna sulfur emissions on the atmospheric composition and aerosol properties in
581 the central Mediterranean: a statistical analysis over the period 2000-2013 based on observations and Lagrangian
582 modelling, *Atmos. Environ.*, 148, 77-88, 2017.
- 583 Ternon, E., Guieu, C., Lojze-Pilot, M. D., Leblond, N., Bosc, E., Gasser, B., Miquel, J. -C., and Martín, J.: The impact
584 of Saharan dust on the particulate export in the water column of the North Western Mediterranean Sea,
585 *Biogeosciences*, 7(3), 809-826, <https://doi.org/10.5194/bg-7-809-2010>, 2010.
- 586 Usher, C. R., Michel, A. E., and Grassian, V. H.: Reactions on mineral dust, *Chemical Reviews*, 103(12), 4883-4940,
587 2003.
- 588 Vincent, J., Laurent, B., Losno, R., Bon Nguyen, E., Roullet, P., Sauvage, S., Chevaillier, S., Coddeville, P.,
589 Ouboulmane, N., di Sarra, A. G., Tovar-Sánchez, A., Sferlazzo, D. M., Massanet, A., Triquet, S., Morales
590 Baquero, R., Fournier, M., Coursier, C., Desboeufs, K., Dulac, F., and Bergametti, G.: Variability of mineral dust
591 deposition in the western Mediterranean basin and south-east of France, *Atmospheric Chemistry and Physics*,
592 16(14), 8749-8766, <https://doi.org/10.5194/acp-16-8749-2016>, 2016.
- 593 Willey, J. D., Kieber, R. J., Eyman, M. S., and Avery, G. B.: Rainwater dissolved organic carbon: concentrations and
594 global flux, *Global Biogeochemical Cycles* 14(1), 139-148, <https://doi.org/10.1029/1999GB900036>, 2000.
- 595



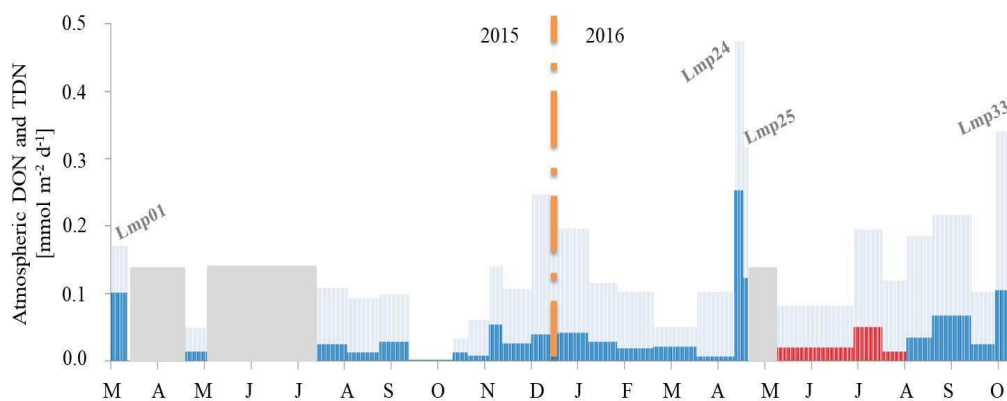
596
597

Figure 1: Lampedusa island (35.5° N, 12.6° E) and the deposition sampler.



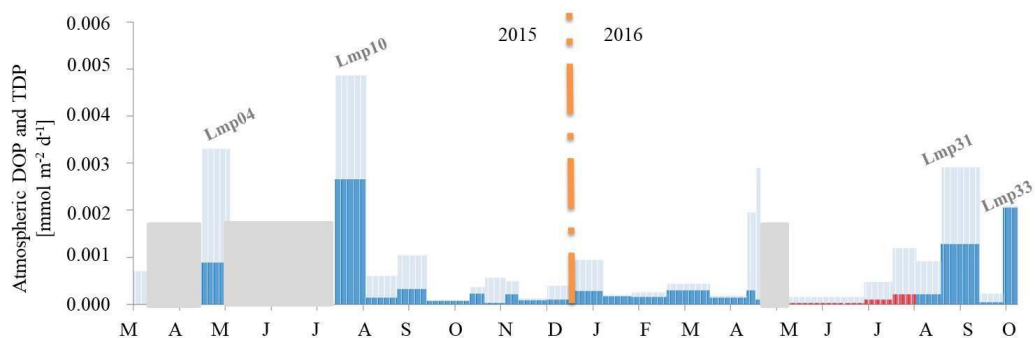
598
 599
 600

Figure 2: Atmospheric DOC fluxes during the study period. The sign of the months is reported every 31 days.



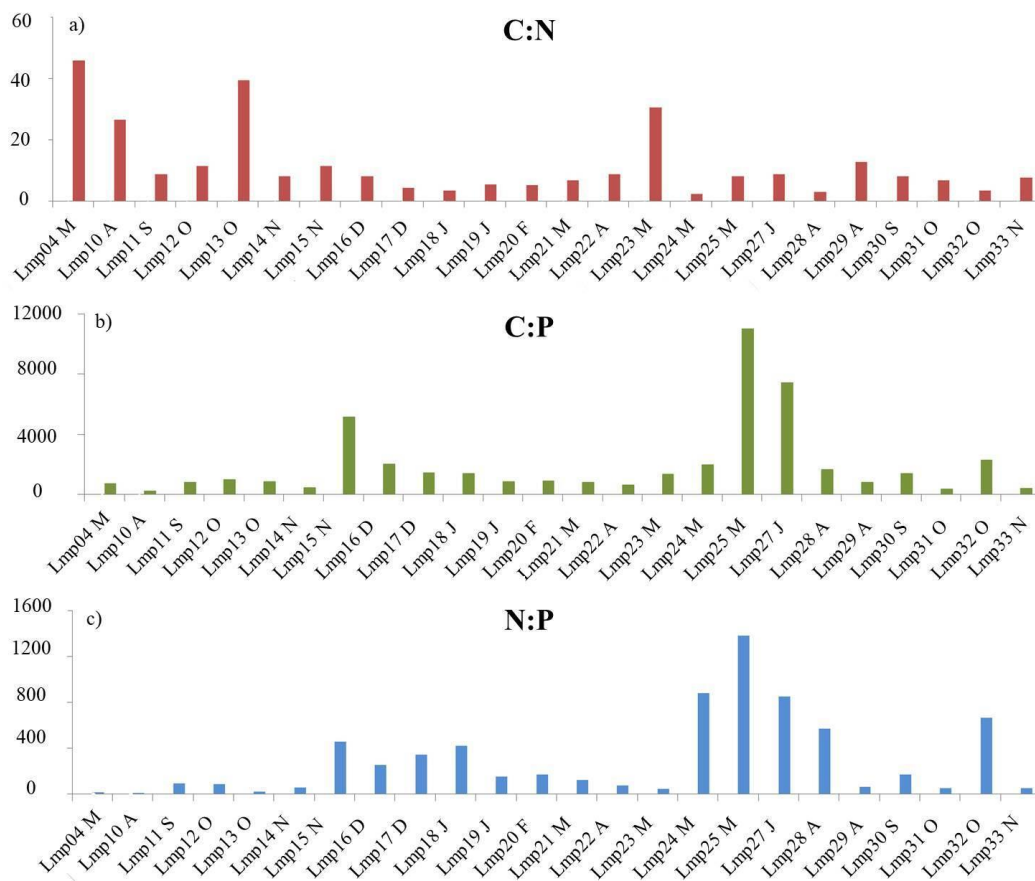
601
 602
 603

Figure 3. Atmospheric DON in blue (wet and dry deposition) and red (dry deposition), and TDN in cyan. No data are available in the grey areas.



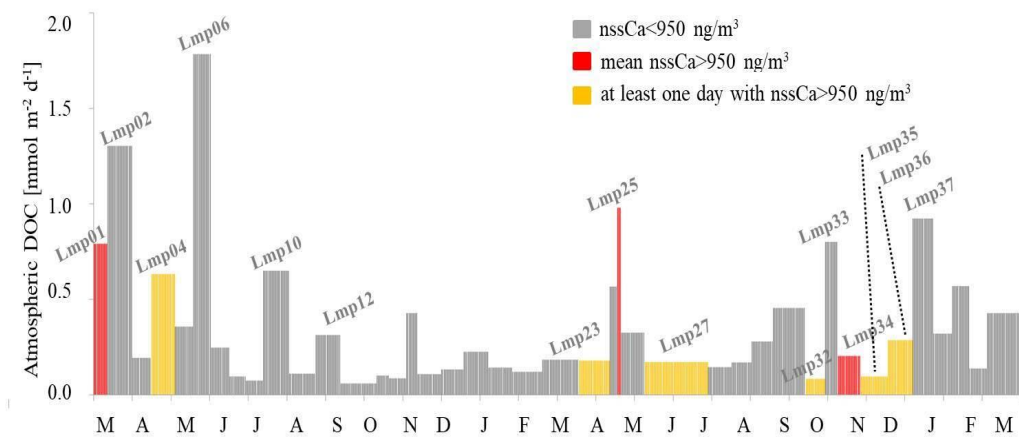
604
605
606
607

Figure 4. Atmospheric DOP in blue (wet and dry deposition) and red (dry deposition), and TDP in cyan. No data are available in the grey areas.



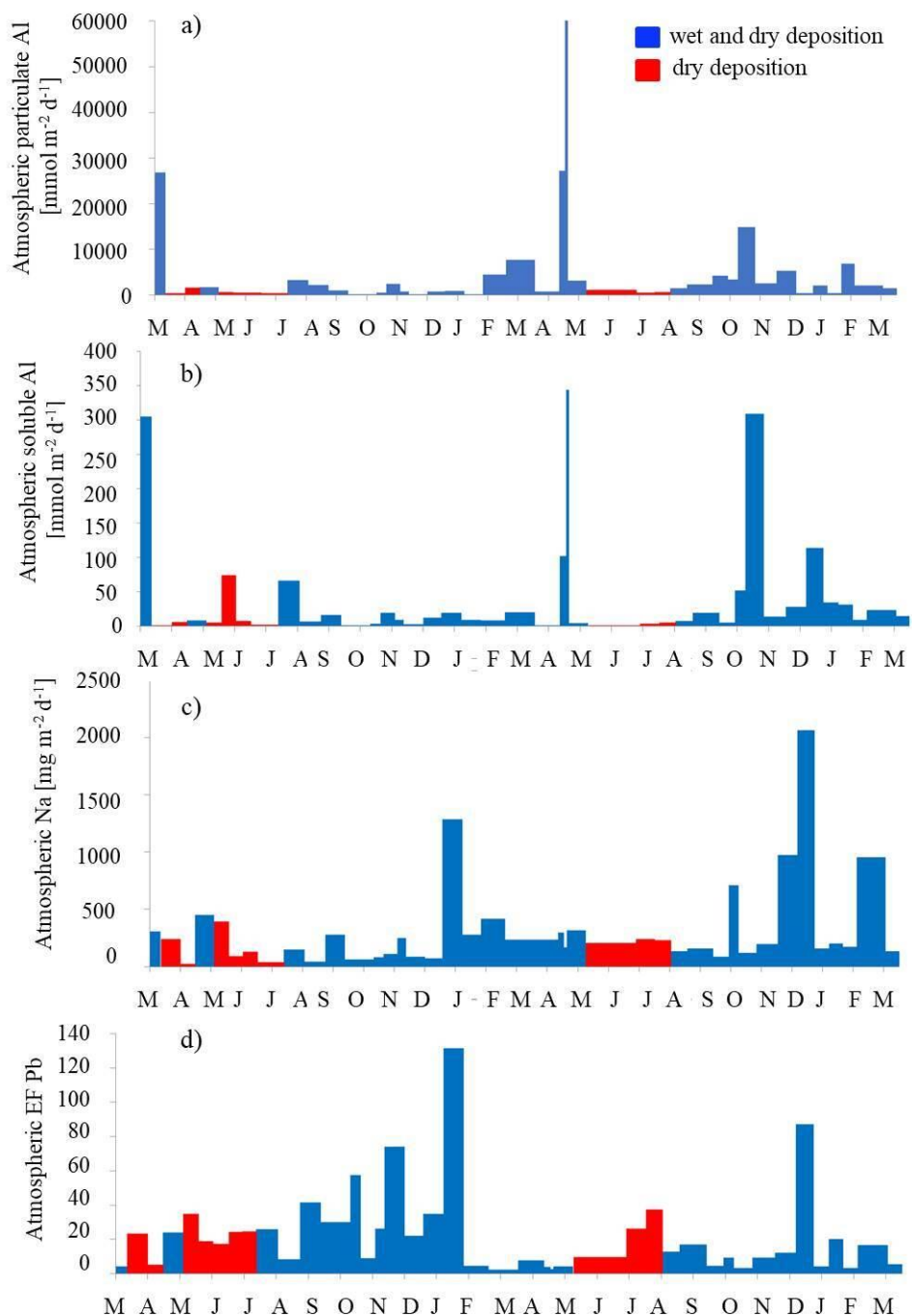
608
609
610
611

Figure 5. Temporal evolution of C:N (a), C:P (b) and N:P (c) ratios. Sample name and the capital letter of the corresponding month of the sampling (from March, Lmp04, to November, Lmp33) are reported in the horizontal axis.



612
613
614

Figure 6. Intensity of dust deposition events during the sampling period based on non-sea salt Ca (nssCa) values.



615
 616 **Figure 7. Atmospheric particulate Aluminium (a), soluble Aluminium (b), soluble Sodium (c) and enrichment**
 617 **factor of Lead (d).**
 618



Sample name	Sampling period			Deposition type	Volume collected [L]
	Start date	End date	Total days		
Lmp01	18/03/2015	28/03/2015	10	wet and dry	6
Lmp02	28/03/2015	17/04/2015	20	dry	0.26
Lmp03	17/04/2015	02/05/2015	16	dry	0.27
Lmp04	02/05/2015	21/05/2015	19	wet and dry	1.8
Lmp05	21/05/2015	05/06/2015	15	dry	0.28
Lmp06	05/06/2015	19/06/2015	15	dry	0.29
Lmp07	19/06/2015	04/07/2015	16	dry	0.26
Lmp08	04/07/2015	17/07/2015	14	dry	0.26
Lmp09	17/07/2015	31/07/2015	14	dry	0.27
Lmp10	31/07/2015	21/08/2015	20	wet and dry	9
Lmp11	21/08/2015	11/09/2015	22	wet and dry	2
Lmp12	11/09/2015	01/10/2015	20	wet and dry	5
Lmp13	01/10/2015	30/10/2015	29	wet and dry	0.5
Lmp14	30/10/2015	09/11/2015	11	wet and dry	2
Lmp15	09/11/2015	23/11/2015	14	wet and dry	0.6
Lmp16	23/11/2015	02/12/2015	9	wet and dry	1.2
Lmp17	02/12/2015	21/12/2015	19	wet and dry	1.9
Lmp18	21/12/2015	08/01/2016	18	wet and dry	1.8
Lmp19	08/01/2016	28/01/2016	20	wet and dry	6.1
Lmp20	28/01/2016	16/02/2016	19	wet and dry	2.7
Lmp21	16/02/2016	11/03/2016	26	wet and dry	2.1
Lmp22	11/03/2016	09/04/2016	28	wet and dry	7.1
Lmp23	09/04/2016	04/05/2016	26	wet and dry	0.3
Lmp24	04/05/2016	10/05/2016	6	wet and dry	2.3
Lmp25	10/05/2016	13/05/2016	3	wet and dry	1.9
Lmp26	13/05/2016	01/06/2016	19	wet and dry	0.7
Lmp27	01/06/2016	22/07/2016	50	dry	0.26
Lmp28	22/07/2016	10/08/2016	19	dry	0.24
Lmp29	10/08/2016	26/08/2016	16	dry	0.24
Lmp30	26/08/2016	12/09/2016	17	wet and dry	0.8
Lmp31	12/09/2016	08/10/2016	26	wet and dry	12
Lmp32	08/10/2016	24/10/2016	16	wet and dry	0.5
Lmp33	24/10/2016	03/11/2016	10	wet and dry	11
Lmp34	03/11/2016	21/11/2016	18	wet and dry	12
Lmp35	21/11/2016	13/12/2016	22	wet and dry	1.7
Lmp36	13/12/2016	02/01/2017	20	wet and dry	9.5
Lmp37	02/01/2017	19/01/2017	17	wet and dry	6.5
Lmp38	19/01/2017	03/02/2017	15	wet and dry	1.5
Lmp39	03/02/2017	17/02/2017	14	wet and dry	5
Lmp40	17/02/2017	03/03/2017	14	wet and dry	0.75
Lmp41	03/03/2017	01/04/2017	29	wet and dry	5.5



619 **Table 1. Sampling period, type of deposition and volume for the 41 samples collected at the Island of**
620 **Lampedusa.**

621



Sample name	DOC fluxes [mmol m ⁻² d ⁻¹]	DON fluxes [mmol m ⁻² d ⁻¹]	TDN fluxes [mmol m ⁻² d ⁻¹]	DOP fluxes [mmol m ⁻² d ⁻¹]	TDP fluxes [mmol m ⁻² d ⁻¹]
Lmp01	0.80	0.10	0.17	0	7·10 ⁻⁴
Lmp02	1.30	n.a.	n.a.	n.a.	n.a.
Lmp03	0.19	n.a.	n.a.	n.a.	n.a.
Lmp04	0.63	0.01	0.05	9·10 ⁻⁴	3·10 ⁻³
Lmp05	0.36	n.a.	n.a.	n.a.	n.a.
Lmp06	1.78	n.a.	n.a.	n.a.	n.a.
Lmp07	0.25	n.a.	n.a.	n.a.	n.a.
Lmp08	0.10	n.a.	n.a.	n.a.	n.a.
Lmp09	0.07	n.a.	n.a.	n.a.	n.a.
Lmp10	0.65	0.02	0.11	3·10 ⁻³	5·10 ⁻³
Lmp11	0.11	0.01	0.09	1·10 ⁻⁴	6·10 ⁻⁴
Lmp12	0.31	0.03	0.10	3·10 ⁻⁴	1·10 ⁻³
Lmp13	0.06	1.5·10 ⁻³	1.6·10 ⁻³	7·10 ⁻⁵	8·10 ⁻⁵
Lmp14	0.10	0.01	0.03	2·10 ⁻⁴	4·10 ⁻⁴
Lmp15	0.09	8·10 ⁻³	0.06	2·10 ⁻⁵	6·10 ⁻⁴
Lmp16	0.43	0.05	0.14	2·10 ⁻⁴	5·10 ⁻⁴
Lmp17	0.11	0.03	0.11	7·10 ⁻⁵	1·10 ⁻⁴
Lmp18	0.13	0.04	0.25	9·10 ⁻⁵	4·10 ⁻⁴
Lmp19	0.23	0.04	0.20	3·10 ⁻⁴	9·10 ⁻⁴
Lmp20	0.14	0.03	0.12	2·10 ⁻⁴	2·10 ⁻⁴
Lmp21	0.12	0.02	0.10	2·10 ⁻⁴	3·10 ⁻⁴
Lmp22	0.18	0.02	0.05	3·10 ⁻⁴	4·10 ⁻⁴
Lmp23	0.18	6·10 ⁻³	0.10	1·10 ⁻⁴	2·10 ⁻⁴
Lmp24	0.57	0.25	0.47	3·10 ⁻⁴	2·10 ⁻³
Lmp25	0.98	0.12	0.32	9·10 ⁻⁵	3·10 ⁻³
Lmp26	0.33	n.a.	n.a.	n.a.	n.a.
Lmp27	0.17	0.02	0.08	2·10 ⁻⁵	1·10 ⁻⁴
Lmp28	0.14	0.05	0.19	9·10 ⁻⁵	5·10 ⁻⁴
Lmp29	0.17	0.01	0.12	2·10 ⁻⁴	1·10 ⁻³
Lmp30	0.28	0.04	0.18	2·10 ⁻⁴	9·10 ⁻⁴
Lmp31	0.45	0.07	0.22	1·10 ⁻³	3·10 ⁻³
Lmp32	0.08	0.02	0.10	4·10 ⁻⁵	2·10 ⁻⁴
Lmp33	0.80	0.10	0.34	2·10 ⁻³	2·10 ⁻³
Lmp34	0.20	n.a.	n.a.	n.a.	n.a.
Lmp35	0.10	n.a.	n.a.	n.a.	n.a.
Lmp36	0.29	n.a.	n.a.	n.a.	n.a.
Lmp37	0.92	n.a.	n.a.	n.a.	n.a.
Lmp38	0.32	n.a.	n.a.	n.a.	n.a.
Lmp39	0.57	n.a.	n.a.	n.a.	n.a.
Lmp40	0.14	n.a.	n.a.	n.a.	n.a.
Lmp41	0.43	n.a.	n.a.	n.a.	n.a.

622 Table 2. Atmospheric fluxes of DOC, DON, TDN, DOP and TDP at the Island of Lampedusa.



623

Sample	Sampling date	C:N	C:P	N:P
Lmp01	28/03/2015	7.78	n.a.	n.a.
Lmp04	21/05/2015	45.87	715.08	15.59
Lmp10	21/08/2015	26.57	244.38	9.20
Lmp11	11/09/2015	8.67	807.94	93.15
Lmp12	01/10/2015	11.37	977.79	85.98
Lmp13	30/10/2015	39.44	864.07	21.91
Lmp14	09/11/2015	8.02	449.04	56.00
Lmp15	23/11/2015	11.26	5131.65	455.83
Lmp16	02/12/2015	7.97	2036.66	255.42
Lmp17	21/12/2015	4.24	1448.37	341.90
Lmp18	08/01/2016	3.34	1406.60	420.55
Lmp19	28/01/2016	5.38	832.69	154.79
Lmp20	16/02/2016	5.09	882.80	173.40
Lmp21	11/03/2016	6.63	812.40	122.55
Lmp22	09/04/2016	8.78	645.65	73.53
Lmp23	04/05/2016	30.48	1353.57	44.41
Lmp24	10/05/2016	2.24	1976.03	882.33
Lmp25	13/05/2016	7.99	11008.94	1377.41
Lmp27	22/07/2016	8.73	7405.29	848.62
Lmp28	10/08/2016	2.89	1641.49	568.76
Lmp29	26/08/2016	12.66	796.68	62.95
Lmp30	12/09/2016	8.06	1376.27	170.77
Lmp31	08/10/2016	6.74	356.03	52.84
Lmp32	24/10/2016	3.41	2275.72	666.53
Lmp33	03/11/2016	7.68	389.57	50.73

624 **Table 3. C:N:P molar ratios in atmospheric DOM.**

625



Sample name	Mean PM ₁₀ [µg/m ³]	Mean sea salt aerosol [µg/m ³]	Mean dust [µg/m ³]	Mean nssCa [ng/m ³]
Lmp01	50.1	13.0	18.2	1327.6
Lmp02	29.0	13.6	n.a.	62.2
Lmp03	28.1	9.8	n.a.	371.6
Lmp04	26.4	8.8	4	351.7
Lmp05	16.7	4.6	n.a.	87.3
Lmp06	23.1	6.1	n.a.	166.1
Lmp07	22.2	7.1	n.a.	139.3
Lmp08	26.5	5.4	n.a.	311.6
Lmp09	28.3	8.0	n.a.	188.2
Lmp10	29.1	5.2	3.4	492.7
Lmp11	n.a.	n.a.	n.a.	n.a.
Lmp12	n.a.	n.a.	n.a.	n.a.
Lmp13	n.a.	n.a.	n.a.	n.a.
Lmp14	n.a.	n.a.	n.a.	n.a.
Lmp15	n.a.	n.a.	n.a.	n.a.
Lmp16	n.a.	n.a.	n.a.	n.a.
Lmp17	n.a.	n.a.	n.a.	n.a.
Lmp18	n.a.	n.a.	n.a.	n.a.
Lmp19	n.a.	n.a.	n.a.	n.a.
Lmp20	n.a.	n.a.	n.a.	n.a.
Lmp21	n.a.	n.a.	n.a.	n.a.
Lmp22	n.a.	n.a.	n.a.	n.a.
Lmp23	39.5	18.3	3.8	488.1
Lmp24	30.7	18.7	1.2	154
Lmp25	133.7	15.5	42.5	4815.1
Lmp26	25.9	13.1	1.5	168.8
Lmp27	26.2	9.3	2.3	319.5
Lmp28	24.7	8.8	1.8	161.5
Lmp29	25	9.6	1.0	235.9
Lmp30	22.4	5.1	n.a.	330.8
Lmp31	24.5	5.6	n.a.	286.2
Lmp32	32.9	8.7	n.a.	772.5
Lmp33	31.8	11.8	n.a.	344.2
Lmp34	35.3	7.8	n.a.	1092.2
Lmp35	22.3	7.5	0.4	394
Lmp36	35.8	12.3	4.6	661.5
Lmp37	n.a.	n.a.	n.a.	n.a.
Lmp38	n.a.	n.a.	n.a.	n.a.
Lmp39	n.a.	n.a.	n.a.	n.a.
Lmp40	n.a.	n.a.	n.a.	n.a.



Lmp41	n.a.	n.a.	n.a.	n.a.
-------	------	------	------	------

626 **Table 4. The PM₁₀, sea salt aerosol, dust and non-sea salt Ca (nss Ca) mean values of the atmospheric DOC**
627 **deposition.**